Journal of Peptide Science
J. Peptide Sci. 2006; **12**: 396–402
Published online 19 December 2005 in Wiley InterScience (www.interscience.wiley.com). DOI: 10.1002/psc.740

JOURNAL OF PEPTIDE SCIENCE

Formation of oriented polypeptides on Au(111) surface depends on the secondary structure controlled by peptide length

TOSHIHIKO SAKURAI,[a]* SAYAKA OKA,[b] ATSUSHI KUBO,[b] KATSUHIKO NISHIYAMA[b] and ISAO TANIGUCHI[b]

[a] Department of Biotechnology, Faculty of Engineering, Tottori University, Tottori 680-8552, Japan
[b] Department of Applied Chemistry and Biochemistry, Faculty of Engineering, Kumamoto University, Kumamoto 860-8555, Japan

Received 15 August 2005; *Revised 28 October 2005*; *Accepted 1 November 2005*

Abstract: We synthesized three different lengths of poly(L-lysine) containing an -SH group at the terminal (PLL_n-SH, n (polymerization degree) = 4, 10, 30) and adsorbed them on an Au(111) surface. To analyze the formation process and the structure of self-assembled monolayers (SAMs), we used atomic force microscopy (AFM) and Fourier transform infrared reflection absorption spectra (FT-IR RAS). At the initial stage of SAM growth, formation of nanosize domains was confirmed by AFM imaging. The α-helical PLL_{30}-SH exhibited a well-defined SAM structure after adsorption reached equilibrium. The α-helical PLL_{30}-SH was almost perpendicular to the gold surface and exhibited interesting molecular packing due to the secondary structure of PLL_{30}-SH and the underlying Au(111) array. The tilt angle of the helix axis from the substrate normal was estimated to be about 50° (AFM) and 44° (FT-IR RAS) respectively. On the other hand, PLL_4-SH and PLL_{10}-SH formed β-sheet-type SAMs on the Au(111) surface based on the structure determined by FT-IR RAS spectrum. Copyright © 2005 European Peptide Society and John Wiley & Sons, Ltd.

Keywords: poly(L-lysine); self-assembled monolayer (SAM); atomic force microscopy (AFM); Fourier transform infrared reflection absorption spectra (FT-IR RAS); α-helical structure; β-sheet structure

INTRODUCTION

For two-dimensional integration of molecules, a wide range of uses as functional interface has been considered including applications such as sensing and surface property modification [1–3]. Therefore, there is a need for precision control over the chemical structure of molecules to contribute to the functionality of the two-dimensional integration. In order to construct the structure, the formation of self-assembled monolayer (SAM) with the thiol group has been reported as a convenient method [4–7]. In each such SAM, it has been shown that the intermolecular interaction and the molecules–substrate interactions effect cooperatively and/or interactively to form a highly ordered monolayer structure. This suggests that a novel SAM structure becomes possible by positively incorporating a noncovalent bonding site in a molecular chemical structure, such as a coordinate-bonding and hydrogen-bonding site. However, many problems affect self-organization of molecules into a structure: e.g. the molecular chemical structure, organizational dynamics, the method of evaluation, and immobilization of the SAM.

In this study, we synthesized three different length polypeptides containing a -SH group at the terminal. These polypeptides have many properties such as a secondary structure, optical activity, and macrodipole–moment interactions. We believe that using a polypeptide not only provides structural information to the SAMs more precisely but also derives the potential for novel functional interfaces such as aligned thin films and chemical sensors. The synthesized polypeptides were adsorbed on an Au(111) surface in order to characterize their structure and the formation process of SAMs on the Au(111) surface through the use of atomic force microscopy (AFM) and Fourier transform infrared reflection absorption spectrum (FT-IR RAS). We discuss the correlation between the degree of polymerization and the assembled surface structure, and the molecular orientation within the self-assembled molecular layer.

MATERIALS AND METHODS

Solid Phase Peptides Synthesis

Three different lengths of poly(L-lysine) with a -SH moiety at the terminal (PLL_n-SH; Figure 1) were prepared by a peptide synthesizer (P. Biosystems, Pioneer) according to the Fmoc solid phase method [8]. This was carried out on a 0.1-mmol scale using the continuous flow method. Side-chain protection was afforded by trityl for *cys*- and *tert*-butoxycarbonyl for Lys. After the final step of deprotection, the resin was dried with 2-propanol. The peptide was cleaved and deprotected by 2.5-h treatment with trifluoroacetic acid (TFA)/water = 95 : 5 (vol%). It was concentrated *in vacuo* and then added to diethylether. The precipitate was collected by filtration and dried *in vacuo*,

*Correspondence to: T. Sakurai, Department of Biotechnology, Faculty of Engineering, Tottori University, Tottori 680-8552, Japan;
e-mail: sakurai@bio.tottori-u.ac.jp

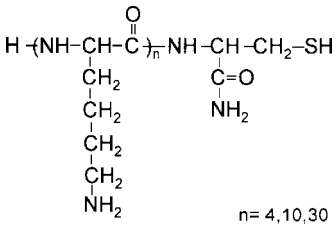

Figure 1 Chemical structure of poly(L-lysine) with thiol group at the terminal.

and a white powder obtained by freeze-drying from a pH 7.0 aqueous solution.

CD Measurement

The circular dichroism (CD) spectra of the polypeptides were measured in trifluoroethanol (TFE) solutions at 20 °C on a JUSCO J-720 CD spectropolarimeter using an optical cell of 1.0 cm path length. The percent of the α-helical contents (f_α) were calculated from Eqn (1) [9].

$$f_\alpha = \frac{([\theta]_{222} + 2000) \times 100}{-30\,000} \quad (1)$$

$[\theta]_{222}$: molar ellipticity of polypeptides at 222 nm.

Preparation of SAM on Au(111) Surface

The Au(111) substrate was prepared by evaporation of gold (99.999%) onto a freshly cleaved mica surface in a homemade vacuum chamber. Evaporation was carried out under previously described conditions where the substrate temperature was kept constant at 300 °C and the pressure in the vacuum chamber was kept at $10^{-6} \sim 10^{-7}$ torr during evaporation [10–12]. After evaporation, the substrate was annealed at 350 °C for 3 h. After cooling the substrate to room temperature, it was treated by flame annealing and immersed directly into TFE solution of PLL_n-SH to be concentrated to 1.0 mM. The Au(111) substrates were immersed into PLL_n-SH/TFE solutions for 1 h at 20 °C. The substrate was quickly removed from the solution and immediately rinsed with enough TFE and dried with N_2 gas.

FT-IR RAS Measurement

The FT-IR refraction adsorption spectra of PLL_n-SH on Au(111) were recorded on a Bio-Rad FTS-6000 Fourier transform infrared spectrometer, and a *p*-polarized beam was obtained through a polarizer. The spectrometer was purged with N_2, and a liquid-nitrogen-cooled mercury–cadmium–telluride (MCT) detector was used for the reflection measurement. The spectra were recorded at a 4 cm^{-1} resolution with 256 scans. We used a Au(111) surface for background measurement in order to minimize the experimental error.

AFM Measurement

The AFM system used in this study was a NanoScope IIIa (Digital Instruments Inc.). The measurements were performed in the tapping and contact modes (15-μm scanner) in air at room temperature. For the tapping mode measurement, we used Si cantilevers (Nanoprobe NCH-10T, Digital Instruments) with a length of 125 μm. For contact mode measurements, we used a Si_3N_4 cantilever with a spring constant of 0.12 N m^{-1} (Nanoprobe NP-S, Digital Instruments) for molecular resolution imaging. All the images were collected in the 'height mode', which kept the force constant. In order to minimize drift effect, the system was calibrated for $6 \sim 8$ h using a standard mica sample. Images shown in this paper were flattened and plane fitted, but not further manipulated. To determine the thickness of the molecular membrane, the images were analyzed with the 'Fractal Analysis' program supplied by Digital Instruments.

RESULTS AND DISCUSSION

CD Measurements

Figure 2 shows the CD spectra of PLL_n-SH in TFE at 20 °C. From the CD spectrum of PLL_4-SH, it can be seen that PLL_4-SH mainly forms a random-coil structure in TFE solution at 20 °C. In contrast, the spectra of PLL_{10}-SH and PLL_{30}-SH in TFE show coexisted spectra of the α-helical and random conformations. The α-helix structure has an extrernum at 208 nm equal to approximately $-30\,000$ deg cm^2 $dmol^{-1}$. For the first approximation, the percent of the α-helix can be calculated from Eqn (1), the α-helical content of PLL_{10}-SH and PLL_{30}-SH were estimated to be about 13 and 90% respectively. Furthermore, the spectrum of PLL_4-SH indicated that PLL_4-SH mainly formed a random-coil structure in the TFE solution. These results indicate that the negative intensity of the molar ellipticity of PLL_n-SH increased at 222 nm, corresponding to an increase in the degree of polymerization, i. e. the chain length of PLL_n-SH stabilized the α-helical conformation. Furthermore, in the case of PLL_{30}-SH, the two negative peaks at 208 and 222 nm that are characteristic of an α-helical structure show that the

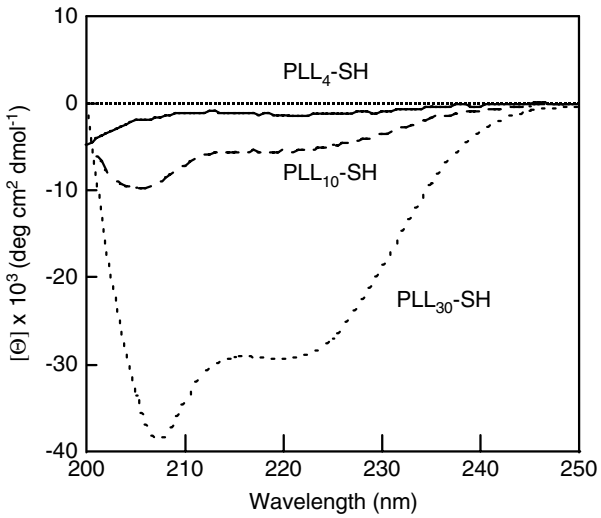

Figure 2 Circular dichroism spectra of PLL_n-SH in TFE solution at 20 °C.

α-helical polypeptides exist in a dispersed state in TFE solutions [13,14].

FT-IR RAS Measurements

Figures 3–5 show *p*-polarized FT-IR RAS of PLL_n-SH adsorbed on Au(111) surfaces. From this spectrum of two peaks, we can postulate that the secondary structure of PLL_n-SH corresponds to the amide I and the amide II bands. Significant differences are observed for the amide bands between the $PLL_{4,10}$-SH spectrum (Figures 3 and 4) and the PLL_{30}-SH spectrum shown in Figure 5. The amide band positions for PLL_4-SH (amide I = 1687 cm^{-1}, amide II = 1514 cm^{-1}) and PLL_{10}-SH (amide I = 1684 cm^{-1}, amide II = 1521 cm^{-1}) prepared from a 1.0-mM TFE solution for 1 h at room temperature have been attributed to a β-sheet structure on an Au(111) surface [15–17]. On the other hand, the peaks of the PLL_{30}-SH corresponding to the amide I and amide II bands were observed at around 1660 and 1546 cm^{-1} respectively. This indicated that the peptide was in α-helical conformation on the Au(111) surface and the difference in the intensity ratio between the two peaks (amide I/amide II) can be explained in terms of the orientation of the α-helix peptide on the gold substrate (Scheme 1). The intensity ratio ascribed to the transition moment of amide I and amide II increases as the tilt angle from the surface normal becomes smaller. The relationship between the tilt angle and the intensity ratio of amide I/amide II is given by Eqn (2) [18,19].

$$D_{\mathrm{obs}} = \frac{A_{\mathrm{Iobs}}}{A_{\mathrm{IIobs}}} = K\frac{A_{\mathrm{Ical}}}{A_{\mathrm{IIcal}}} = K\frac{2\left[\frac{1}{2}(3\cos^2\theta - 1)\right]\left[\frac{1}{2}(3\cos^2\theta_{\mathrm{I}} - 1)\right] + 1}{2\left[\frac{1}{2}(3\cos^2\theta - 1)\right]\left[\frac{1}{2}(3\cos^2\theta_{\mathrm{II}} - 1)\right] + 1} \quad (2)$$

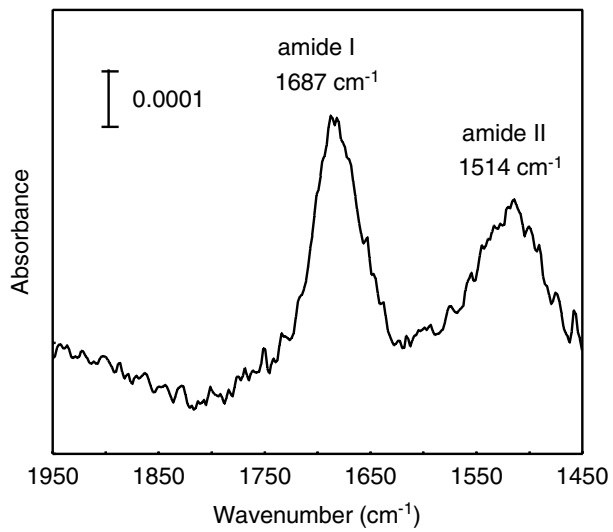

Figure 3 FT-IR RAS spectrum of PLL_4-SH on Au(111) surface.

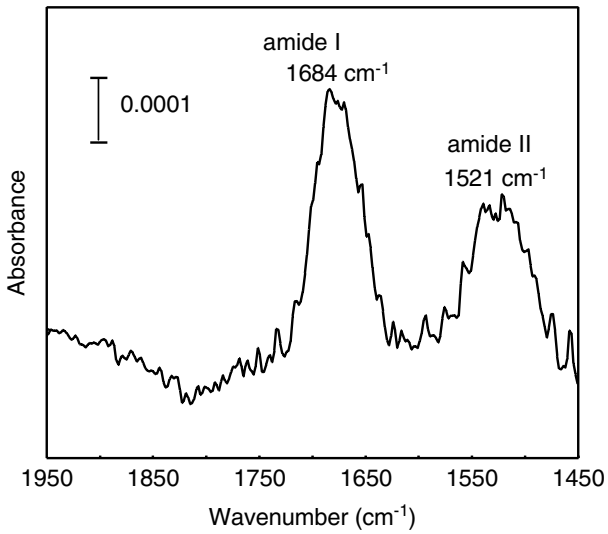

Figure 4 FT-IR RAS spectrum of PLL_{10}-SH on Au(111) surface.

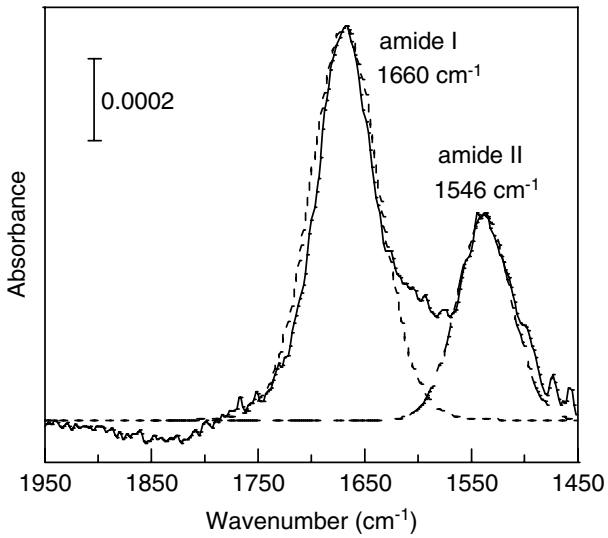

Figure 5 FT-IR RAS spectrum of PLL_{30}-SH on Au(111) surface. The solid line resulted from experimental data. The dotted lines show the amide I and amide II peak area after peak separation.

θ_{I}: the angle between the transition moment of amide I and the axis as 39°.
θ_{II}: the angle between the transition moment of amide II and the axis as 75°.
K: the scaling constant.

To obtain truly quantitative data, Gaussian distribution of the spectrum was used to enhance peak separation and the determination of the peak area. The peak area of the amide I and amide II were estimated to be 0.079 and 0.033 respectively. Hence, intensity ratio (amide I_{obs}/amide II_{obs}) of PLL_{30}-SH SAM was about 2.4. From Eqn (3), the tilt angle was calculated to be about 44° from surface normal. This supports the conclusion

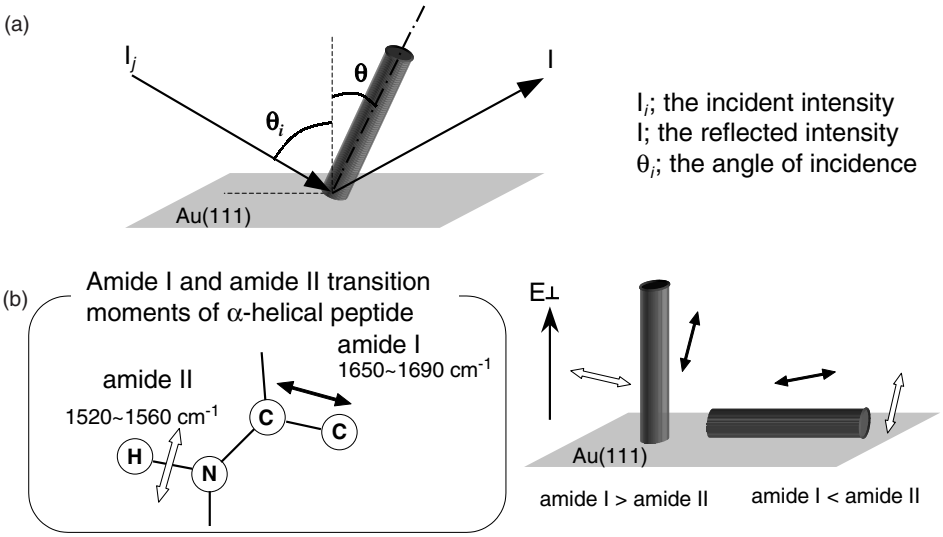

Scheme 1 Schematic illustration of (a) FT-IR RAS measurement and (b) the relationship of amide I and amide II transition moment formed α-helical structure.

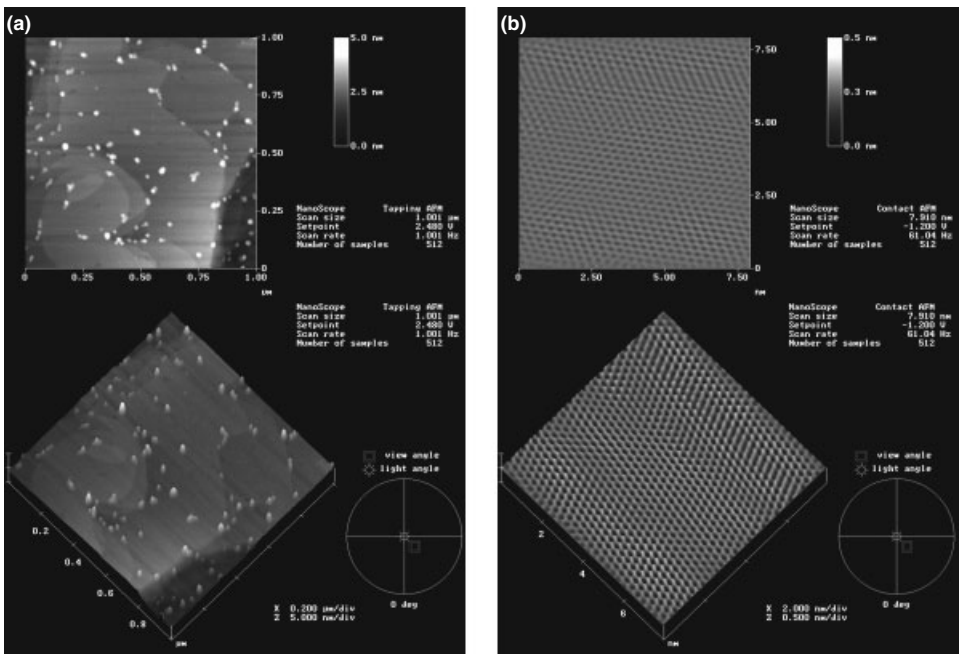

Figure 6 AFM images of Au(111) crystal surface deposited on cleaved mica surface. (a) 1 μm × 1 μm, (b) 8 nm × 8 nm. In the images, the bright regions correspond to the high region and the dark regions correspond to the low region.

that the α-helical PLL_{30}-SH was mostly oriented perpendicular to the surface, as described. In addition, the tilt angle of the PLL_{30}-SH helix axis from the substrate normal decreased with the passage of time for adsorption, and a change of the tilt angle was not observed after 1 h.

Surface Morphology of PLL_n-SH on Au(111) Surface

AFM images of the Au(111)/mica substrates used in this study show that the surface morphology of the substrates consisted of flat terraces (Figure 6a). A higher-resolution image of a terrace revealed a hexagonal pattern of bright spots with nearest neighbor spacing (3.0 ± 0.1 Å), which is consistent with a Au(111) lattice (Figure 6b) [10,11].

The surface morphology of PLL_{30}-SH on Au(111) surface, PLL_{30}-SH formed small domains on the Au(111) surface during the first stage of adsorption. These domains grew to form a homogeneous layer within 1 h, and the Au(111) surfaces were almost covered with molecular layers yielding smooth surfaces (Figure 7c). However, it was also observed that there were several defects in the molecular layers corresponding to

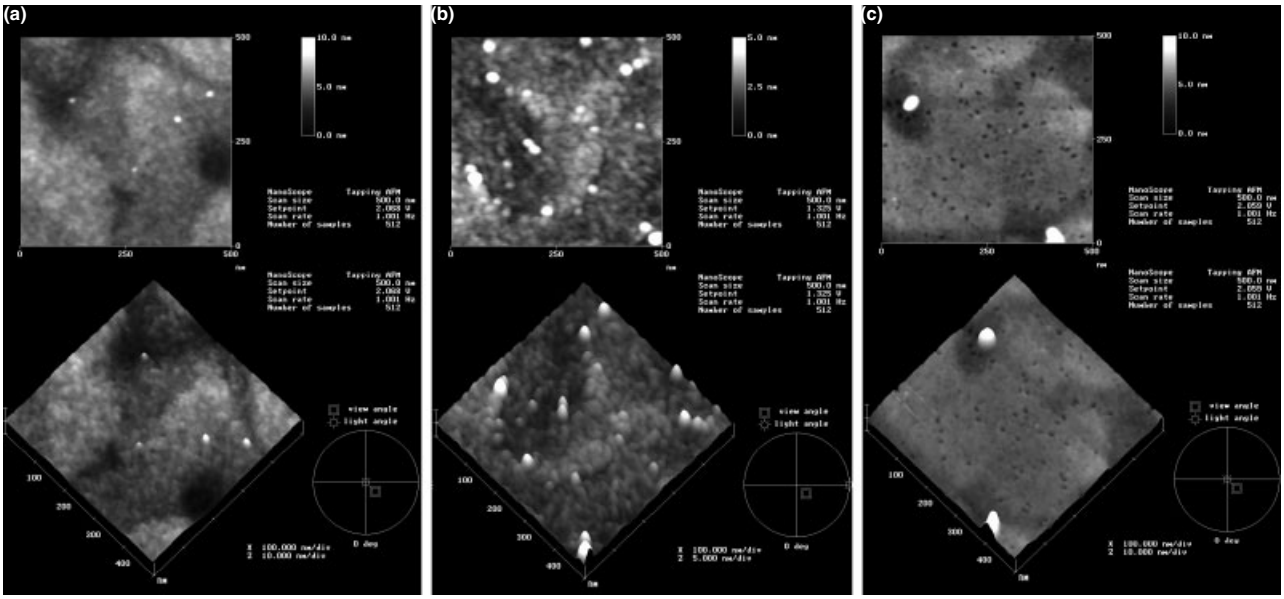

Figure 7 AFM images of PLL_n-SH on Au(111) in 1.0 mM TFE solution for 1 h. (a) PLL_4-SH, (b) PLL_{10}-SH, (c) PLL_{30}-SH.

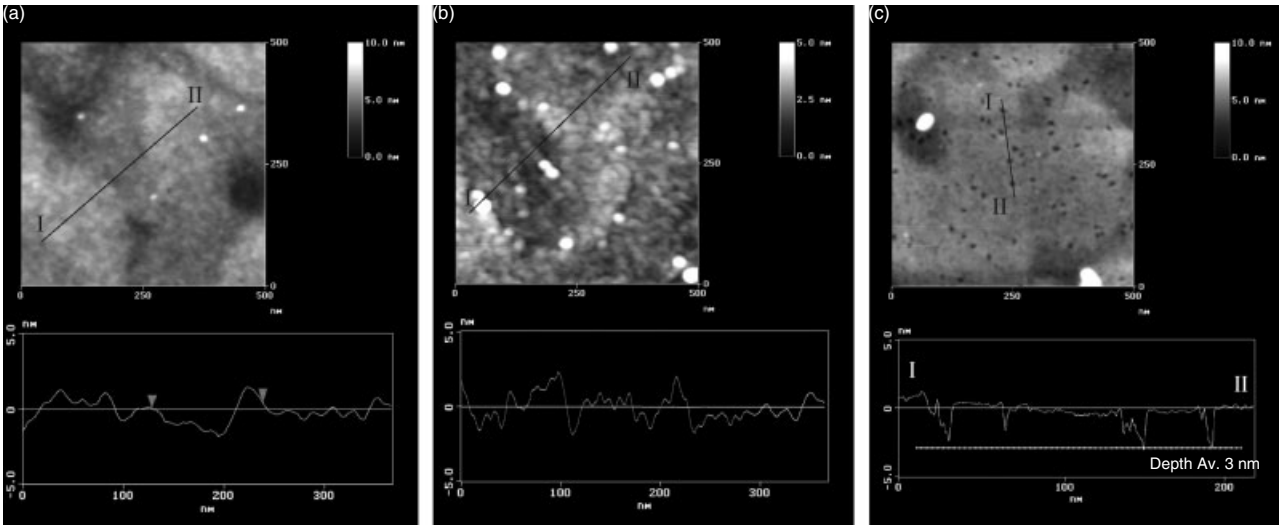

Figure 8 AFM images of PLL_n-SH on Au(111) and cross-sectional profile along the line draw on image. (a) PLL_4-SH, (b) PLL_{10}-SH, (c) PLL_{30}-SH.

the pure Au(111) surface. The difference in height between the smooth surface and the pure Au(111) surfaces provided an estimate of the molecular layer thickness, which was found to be approximately 3.0 nm (Figure 8c). From this distance and the length of PLL_{30}-SH when forming a perfect α-helical structure (4.8 nm) as estimated using the CPK models derived from PEPCON (Figure 9a), we can estimate the tilt angle from the substrate normal, considering the thickness of the monolayer and the length of the α-helical PLL_{30}-SH, a value of 50° (Figure 9b). The molecular orientation of PLL_{30}-SH in SAM must be influenced by substrate–molecule interactions with respect to the underlying Au(111) surface lattice. In this case, the difference between the diameter of the α-helical PLL_{30}-SH and the distance of the threefold hollow site (the threefold hollow site is the most stable binding site for chemisorptions of a thiol group on Au(111)) causes vacancies among the α-helix rod. Therefore, the α-helical PLL_{30}-SH must form a more closely packed structure at the substrate–air interface to stabilize the vacancies. This causes the tilt of the α-helical rods.

On the other hand, in AFM images of PLL_4-SH and PLL_{10}-SH, we could not observe a homogeneous layer such as a PLL_{30}-SH monolayer (Figure 7a,b). However, from the FT-IR RAS measurements, we concluded that PLL_4-SH and PLL_{10}-SH formed a β-sheet-type SAM on the Au(111) surface. PLL_4-SH and PLL_{10}-SH formed small domains on the Au(111) surface at the first stage

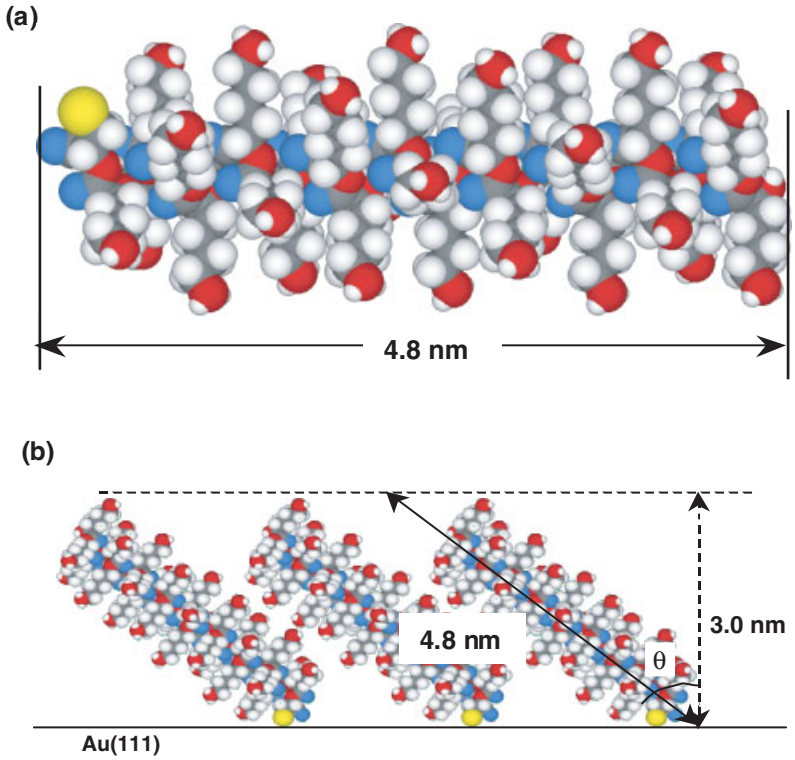

Figure 9 (a) CPK model of α-helical PLL_{30}-SH derived from PEPCON and (b) schematic illustration of α-helical PLL_{30}-SH on Au(111) surface.

of adsorption similar to those seen with PLL_{30}-SH. However, these domains did not grow to a homogeneous layer within 1 h (Figure 8a,b). This could be because of the effects of the secondary structure of polypeptides in TFE solution. PLL_4-SH and PLL_{10}-SH mainly form random-coil structure in TFE solution. Therefore, PLL_4-SH and PLL_{10}-SH did not form rigid molecular structures that would have allowed the construction of a well-defined SAM on the Au(111) surface governed by intermolecular interactions and molecule–substrate interactions. The secondary structure transition to β-sheet structure is probably due to molecular rearrangement. Considering the mobility of the molecules, rearrangement of the molecules seems to have occurred at the physisorption stage before chemisorption resulted in bonding between the thiol group and gold atoms. Because of the intermolecular interactions, PLL_4-SH and PLL_{10}-SH folded into a β-sheet structure at the physisorption stage.

These results indicate that it is possible to construct finely ordered SAMs by making small changes in the peptide, such as the peptide length. Furthermore, the structural features of SAMs constructed from α-helical polypeptides on an Au(111) surface were found to be strongly dependent on factors such as side group interactions and the relationship between the helix structure and underlying Au(111) array. In such a case, we cannot ignore the effect of the solvent used for immersion; however, it was demonstrated that small modifications to the polypeptide molecules changed the intermolecular interactions that govern the structure of SAMs. This enabled us to construct a novel structure of highly ordered SAMs and to demonstrate their utility as new functional interfaces.

CONCLUSIONS

The structures and growth of SAMs using three different lengths of PLL_n-SH on Au(111) were studied by AFM and FT-IR RAS measurements. The structures of the PLL_n-SH SAMs were found to be strongly dependent on the degree of polymerization, i.e. the chain length of the PLL_n-SH. This resulted in differences in the secondary structures in the TFE solution and in the intermolecular interactions during the physisorption stage.

PLL_4-SH and PLL_{10}-SH formed β-sheet structure on Au(111) surface, and α-helical PLL_{30}-SH assembled into well-defined SAMs on Au(111) surface. The structural features of the SAMs were found to be strongly dependent on several factors, including the relationship between the helix structure and the underlying Au(111) array, the effect of the solvent used, and the side group interaction. This appeared to be because the length of PLL_n-SH allowed for the rearrangement of the secondary structure at the physisorption stage; therefore, the intermolecular interaction that causes the assembly of the SAM occurred. These results suggest that the secondary structure of the polypeptide

plays a large role in regulating the structure of SAMs through intermolecular interaction.

REFERENCES

1. Turyan I, Mandler D. Selecive determination of Cr(VI) by a self-assembled monolayer-based electrode. *Anal. Chem.* 1997; **69**: 894–897.
2. Maeda Y, Fukuda T, Yamamoto H, Kitano H. Regio- and stereoselective complexation by a self-assembled monolayer of thiolated cyclodextrin on a gold electrode. *Langmuir* 1997; **13**: 4187–4189.
3. Shundo A, Sakurai T, Takafuji M, Nagaoka S, Ihara H. Molecular-length and chiral discriminations by beta-structural poly(L-alanine) on silica. *J. Chromatogr., A* 2005; **1073**: 169–174.
4. Sellers H, Ulman A, Shnidman Y, Elilers JE. Structure and binding of alkanethiolates on gold and silver surface: implications for self-assembled monolayers. *J. Am. Chem. Soc.* 1993; **115**: 9389–9401.
5. Fujita K, Kimura S, Imanishi Y, Okamura E, Umemura J. Monolayer formation and monolayer orientation of various helical peptides at the air/water interface. *Langmuir* 1995; **11**: 1675–1679.
6. Jaschke M, Schonherr H, Wolf H, Butt HJ, Besocke MK, Ringsdorf H. Structure of alkyl and perfluoroalkyl disulfide and azobenzenthiol monolayers on gold(111) revealed by atomic force microscopy. *J. Phys. Chem.* 1996; **100**: 2290–2301.
7. Sawaguchi T, Mizutani F, Taniguchi I. Direct observation of 4-mercaptopyridine and Bis(4-pyridyl) disulfide monolayers on Au(111) in perchloric acid solution using in situ scanning tunneling microscopy. *Langmuir* 1998; **14**: 3565–3569.
8. Chang CD, Felix AM, Jimenez MH, Meienhofer J. Solid-phase peptide synthesis of somatostatin using mild base cleavage of N-alpha-9-fluorenylmethyloxycarbonylamino acid. *Int. J. Pept. Protein Res.* 1980; **15**: 485–494.
9. Wu C-SC, Ikeda K, Yang JT. Ordered conformation of polypeptides and proteins in acidic dodecyl sulfate solution. *Biochemistry* 1981; **20**: 56–570.
10. Chidsey ED, Loiacono DN, Sleator T, Nakahara S. STM study of the surface morphology of gold on mica. *Surf. Sci.* 1988; **200**: 45–66.
11. Sobotik P, Ost'adal I. Temperature induced change of surface roughness of Au(111) epiaxial films on mica. *J. Cryst. Growth* 1999; **197**: 955–962.
12. Goss CA, Brumfield JC, Irene EA, Murray RW. Imaging and modification of gold(111) monatomic steps with atomic force microscopy. *Langmuir* 1993; **9**: 2986–2994.
13. Holzwarth G, Doty P. The ultraviolet circular dichroism of polypeptides. *J. Am. Chem. Soc.* 1965; **87**: 218–228.
14. Chen YH, Yang JT, Chau KH. Determination of the helixand b form of proteins in aqueous solution by circular dichroism. *Biochemistry* 1974; **13**: 3350–3359.
15. Susi H, Timasheff SN, Stevens L. Infrared spectra and protein conformations in aqueous solution. *J. Biol. Chem.* 1967; **242**: 5460–5466.
16. Jordan CE, Frey BL, Kornguth S, Corn RM. Characterization of poly-L-lysine adsorption onto alkanethiol-modified gold surfaces with polarization-modulation Fourier transform infrared spectroscopy and surface plasmon resonance measurements. *Langmuir* 1994; **10**: 3642–3648.
17. Frey BL, Corn RM. Covalent attachment and derivatization of poly(l-lysine) monolayers on gold surfaces as characterized by polarization-modulation FT-IR spectroscopy. *Anal. Chem.* 1996; **68**: 3187–3193.
18. Gremlich HU, Fringeli UP, Schwyzer R. Conformational changes of adrnocorticotropin peptides upon interaction with lipid membranes revealed by infrared attenuated total reflection spectroscopy. *Biochemistry* 1983; **22**: 4257–4264.
19. Worley CG, Linton RW, Samulski ET. Electric-field-enhanced self-assembly of – alpha, -helical polypeptides. *Langmuir* 1995; **11**: 3805–3810.